

CMS Pixel Simulations

Morris Swartz
Dept. of Physics and Astronomy
Johns Hopkins University
morris@jhu.edu

5 November 2002

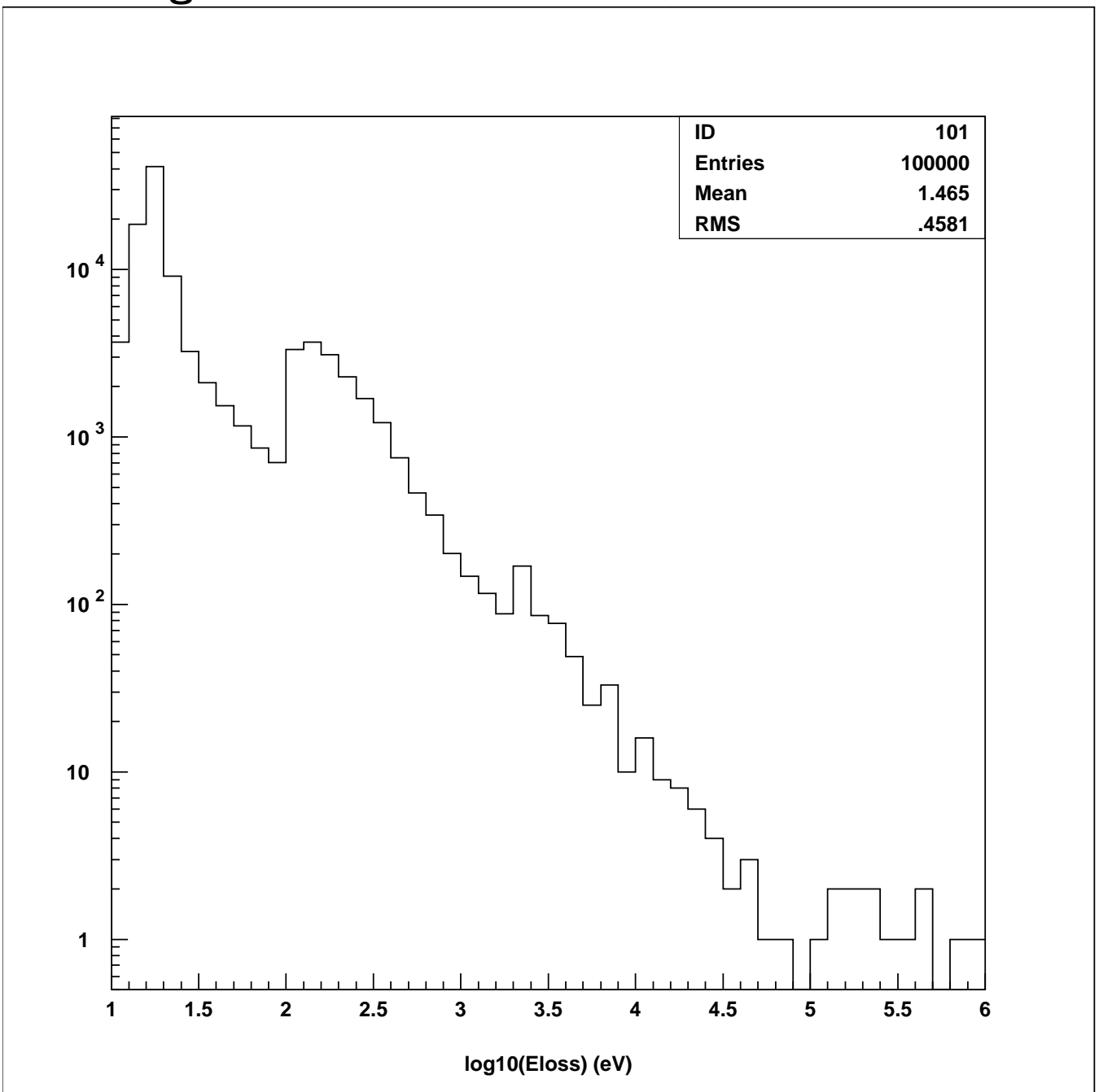
Motivation for Detailed Sensor Simulation

- The “Official” CMS Monte Carlo uses an idealized charge transport model.
- Need something to compare the with the test beam data and to aid in design choices. **Should be more physical and include more realistic effects:**
 - Accurate charge deposition in silicon (delta rays).
 - Realistic electric fields including type inversion effects and limited depletion.
 - Real charge drift physics including mobilities, Hall Effect, and 3D diffusion.
 - Include radiation damage and charge trapping effects.
- Simulation should be useful for understanding actual performance after operation begins and for designing/tuning reconstruction and calibration software.
- Simulation does not have to be fast enough for use in high volume Monte Carlo of CMS data.

Content of this talk can be found in **CMS Note 2002/027**.

Ingredients of Detailed Simulation

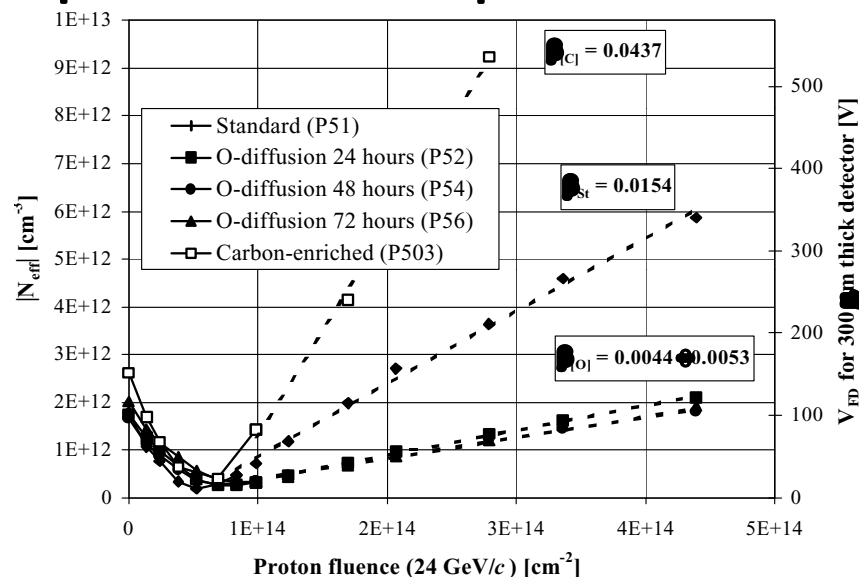
1. “Exact” energy loss via the $\pi - e$ elastic cross sections of H. Bichsel, RMP 60, 663 (1988)
 - Distance to next energy deposition is chosen from an exponential distribution with correct mean free path.
 - Energy loss is chosen between 10 eV and 1 MeV according to correct distribution,



- Secondary e^- are deposited along delta ray tracks:
 - Direction of delta ray chosen according to 2-body kinematics.
 - Secondary e^- are chosen according to Poisson distribution for avg energy per electron of 3.68 eV.
 - Range and e^- density chosen according to empirical range-energy relation.
 - Delta rays followed until all energy is deposited or secondary leaves Si.
- Procedure leads to “exact” energy loss distribution with accurate tails (Landau/Vavilov distributions are approximations to this distribution).

2. Electric fields in sensors are simulated using ATLAS, a very fancy 3-D electrostatic simulation package:

- solves electrostatics using full-blown treatment of charge densities + currents in doped semiconductors
- effective doping densities in irradiated silicon are taken from published RD48 plots



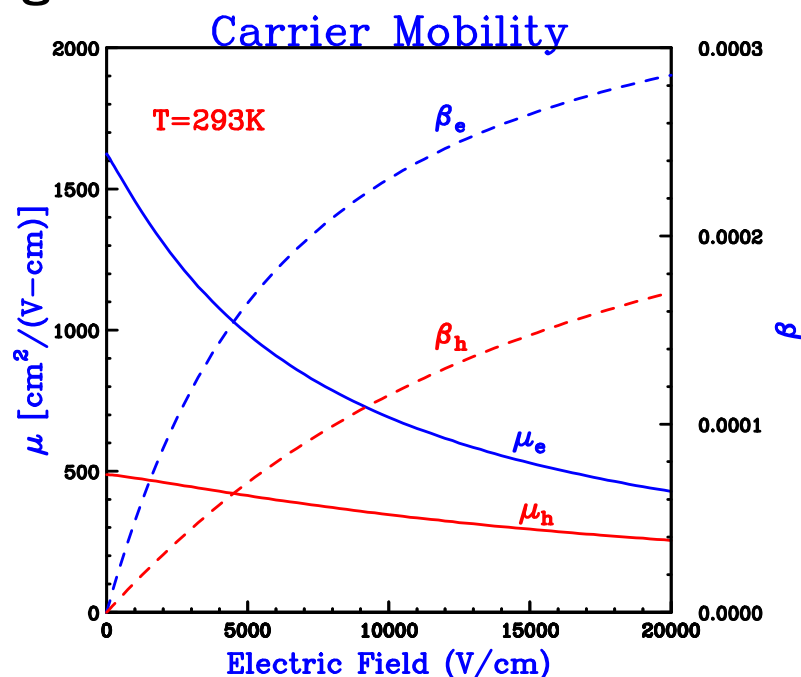
- 3D simulations are SLOW (24 cpu hrs on 500 MHz ultrasparc IIe vs 6.5 min for equivalent 2D sim).
- Assume 4-fold symmetry of each pixel cell to achieve good mesh density and finite execution time:
 - doesn't simulate field distortions due to gaps in p-stop rings

3. Equations of motion for e^- and h are numerically integrated using 5th-order Runge-Kutta method,

$$\frac{d\vec{x}}{dt} = \vec{v}$$

$$\frac{d\vec{v}}{dt} = \frac{e}{m^*} \left[q\vec{E} + qr_H\vec{v} \times \vec{B} - \frac{\vec{v}}{\mu(E)} \right]$$

- m^* for e and h in Si are $0.26 \cdot m_e$ and $0.24 \cdot m_e$
- Mobility $\mu = v_{drift}/E$ is well-characterized for our (low) doping densities



- Hall factor r_H is not well-known. Take $r_H = 1.15$.
- Add 3-d diffusion to the integration. The diffusion length along each projection is

$$\ell_D = \sqrt{D\Delta t} \quad D = \frac{kT}{e}\mu$$

- Unfortunately, the time-step Δt cannot be made larger than the thermalizing time $m^*\mu/e \leq 0.1$ ps (otherwise, solutions become numerically unstable).
 - Simulation is very slow (initially full simulation of one event required 5 cpu hours on an 800 MHz pentium-class processor):
 - Recoding Runge-Kutta loop in-line to avoid function calls and minimizing field lookups gained a factor of 9!
 - Converting code to C and rewriting loop for G4 powerpc vector processor gained a factor of 6-7! Each 500 MHz G4 will execute this code at the same speed as a 5 GHz pentium-class processor. Have two 500 MHz G4's and one 733 MHz G4 available at night.
 - It is not necessary to propagate all 20k-150k electrons from a pixel hit. Following 1/10 gives same result, gains factor of 10!
 - Reduces 5 hours to 30 seconds. With three processors, can simulate 1000 FPix hits in 2.5-3 hours! High η barrel hits can take 8-10 times longer.

4. **Charge trapping:** electrons and holes drifting in radiation-damaged silicon can become trapped for long (> 100 ns) times. They are not promptly collected by the readout electronics (integrating times of approx 35 ns). The trapped charges do “detrap” eventually and do not affect the steady-state electrostatics.

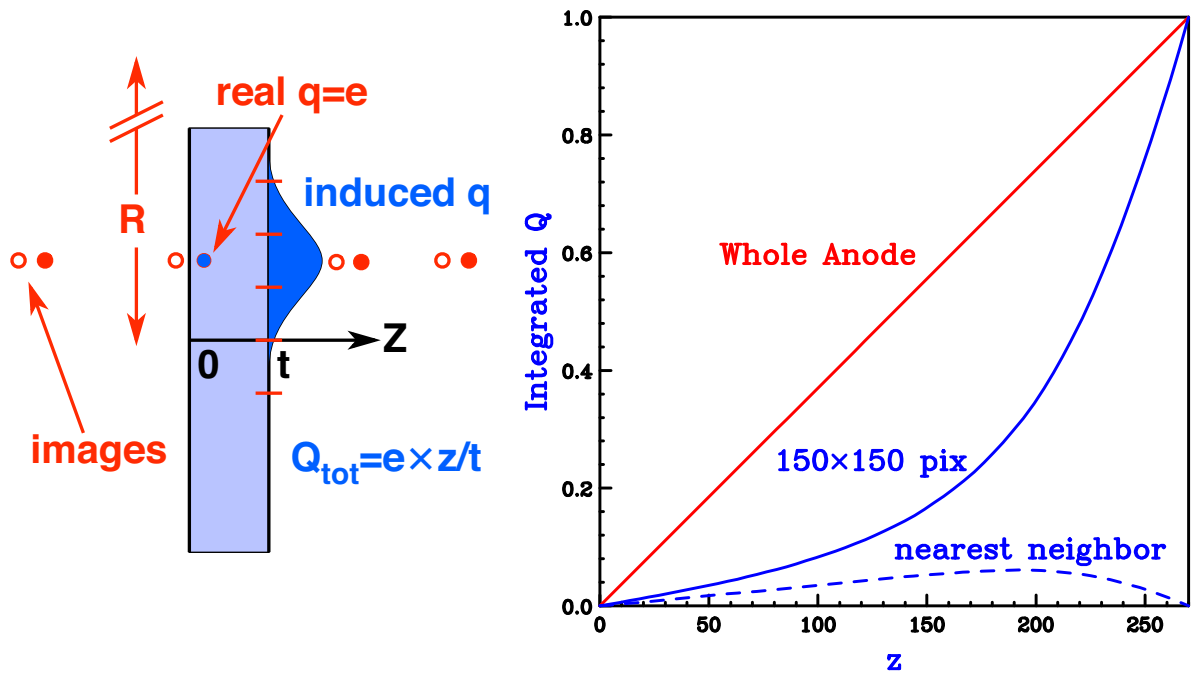
In the last 2 years, Kramberger et al have measured the trapping times [NIM A476, 645 (2002)]. The trapping times are related to trapping probabilities

$$dP = \frac{dt}{\tau_{eff}} = \beta(T)\Phi_{eq} \cdot dt$$

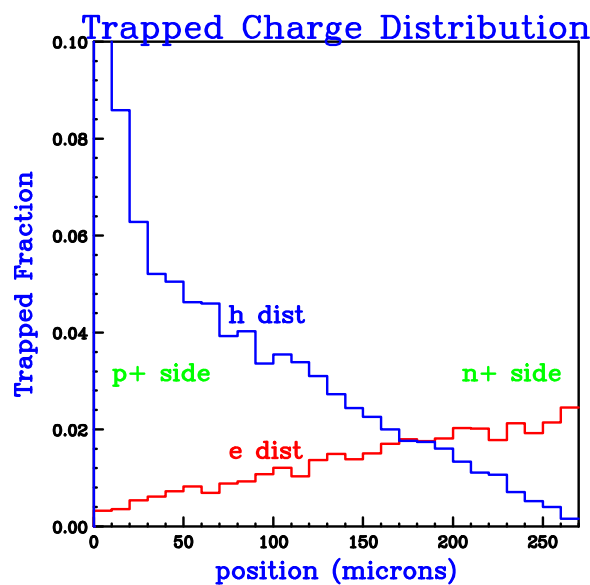
and are expressed as functions of temperature T and hadronic flux Φ_{eq} . In order to correctly include the induced charge effects, we must include hole trapping. The trapping times for holes are very similar to those for electrons but because the mobilities of the holes are typically 1/3 those of the electrons, essentially all of the holes are trapped as compared with about 40% of the electrons in heavily damaged sensors. The simulation:

- Propagates positrons (code originally written to do this anyway) - costs a factor of 2-3 in cpu time
- Ceases propagation of “trapped” charges
- Calculates the signals induced on the n+ implants:
 - assume that a parallel plate capacitor is a valid model (all field lines are “gathered” by the n+ implant)

- sum over first 13 image charges ... the aspect ratio of a pixel cell does not require many images



The distribution of trapped charge across a heavily-damaged (non-oxygenated) sensor looks like this



The excess of trapped electrons near the n+ implant is partly compensated by the trapped positrons. The

induced charges on the neighboring pixels are relatively small and can be of either sign.

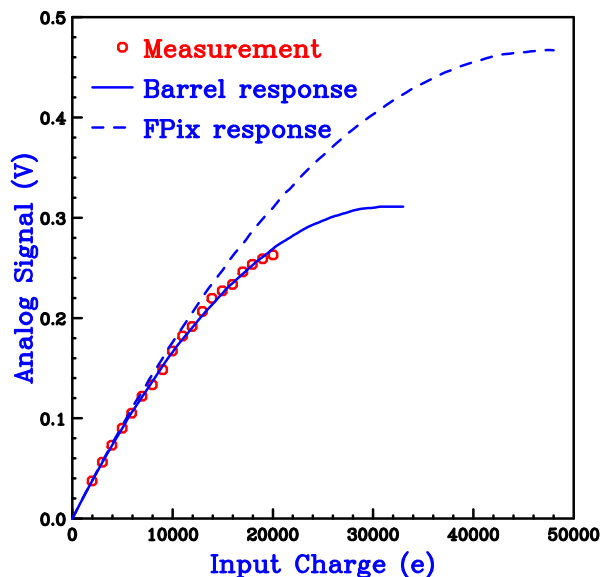
The difference between ignoring the induced signals of the trapped charge and including them is typically 5% of the total signal on the “hit” pixels (pixels with signals larger than the 2000 to 2500 electron threshold).

5. Simulated pixel hits are written to disk as a 13X5 grid of pixel signals

Electronic noise, ROC analog response, digitizer truncation, and threshold effects are added during the analysis phase and can be changed easily.

6. Electronic Response - done in four steps:

- **Noise** - add random noise signal of 500 electrons rms to each pixel signal
- **ROC Analog Response** Simulate the analog response from extrapolated Aachen measurements



which saturates at 33,000 electrons. Try an ad-hoc “improved” response also.

- **Apply readout threshold** Use **5** times noise or **2500** electrons.
- **Digitize simulated ROC output** Assume FED transmits 6 bits of pulse height information.

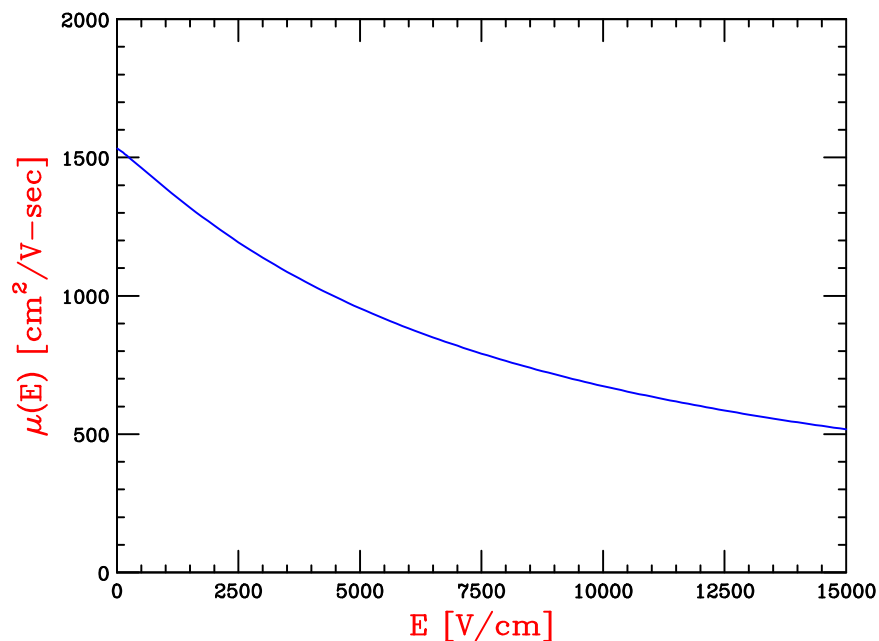
Charge-Sharing Physics

The pixel system resolution depends heavily on the sharing of charge between cells. Sharing in the FPix depends upon geometrical sharing in the ϕ direction and a combination of geometrical and Lorentz drift in the r direction. The barrel relies (heavily) on Lorentz-drift in the ϕ direction and geometrical sharing in the z direction.

A simple approximation for the Lorentz angle (valid for small angles) is

$$\tan \theta_L \simeq \frac{er_H v B \sin \theta_{vB}}{eE} = r_H \mu(E) B \sin \theta_{vB}$$

where the mobility decreases with increasing electric field,

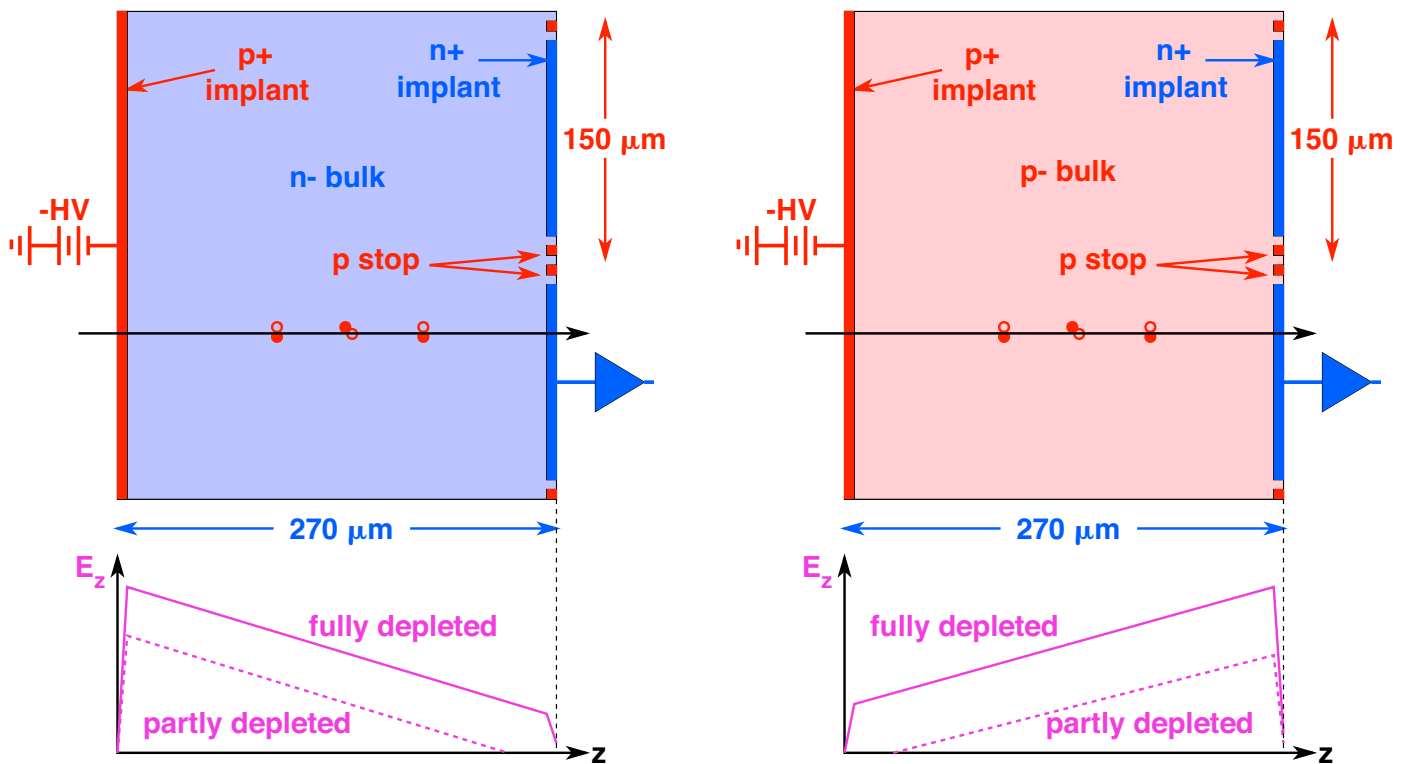


The actual transverse displacement comes from

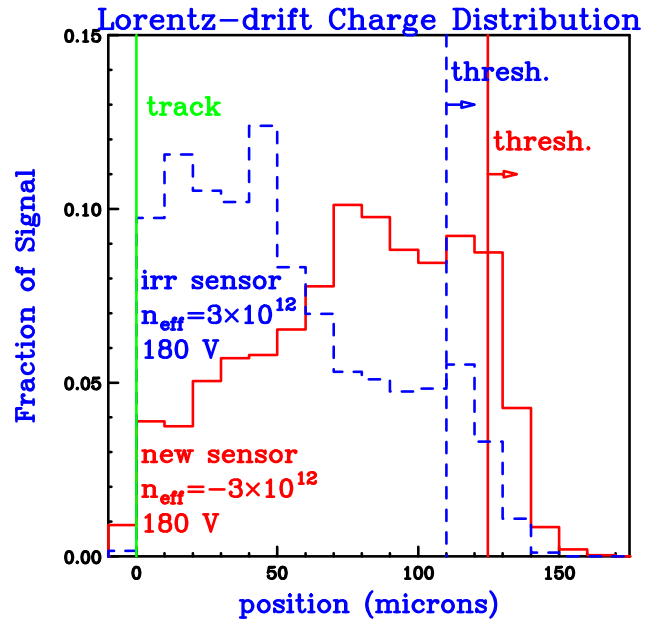
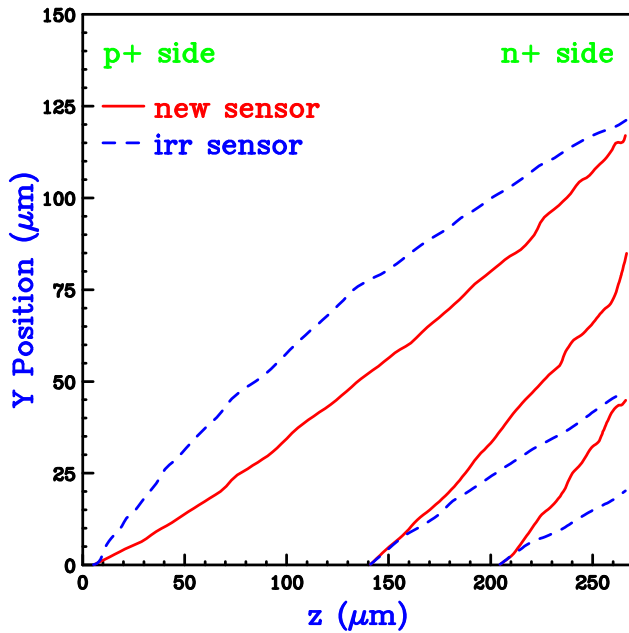
integrating over the entire path,

$$\Delta y = \int_{path} \tan \theta_L dz \simeq \int_{path} r_H \mu(E) B \sin \theta_v B dz$$

The total transverse displacement depends upon the electric field profile over the entire path. To study this, let's consider two diodes: **n-doped at $-3 \times 10^{12} \text{cm}^{-3}$ (new)**, and **p-doped at $+3 \times 10^{12} \text{cm}^{-3}$ (irr)** (no trapping),

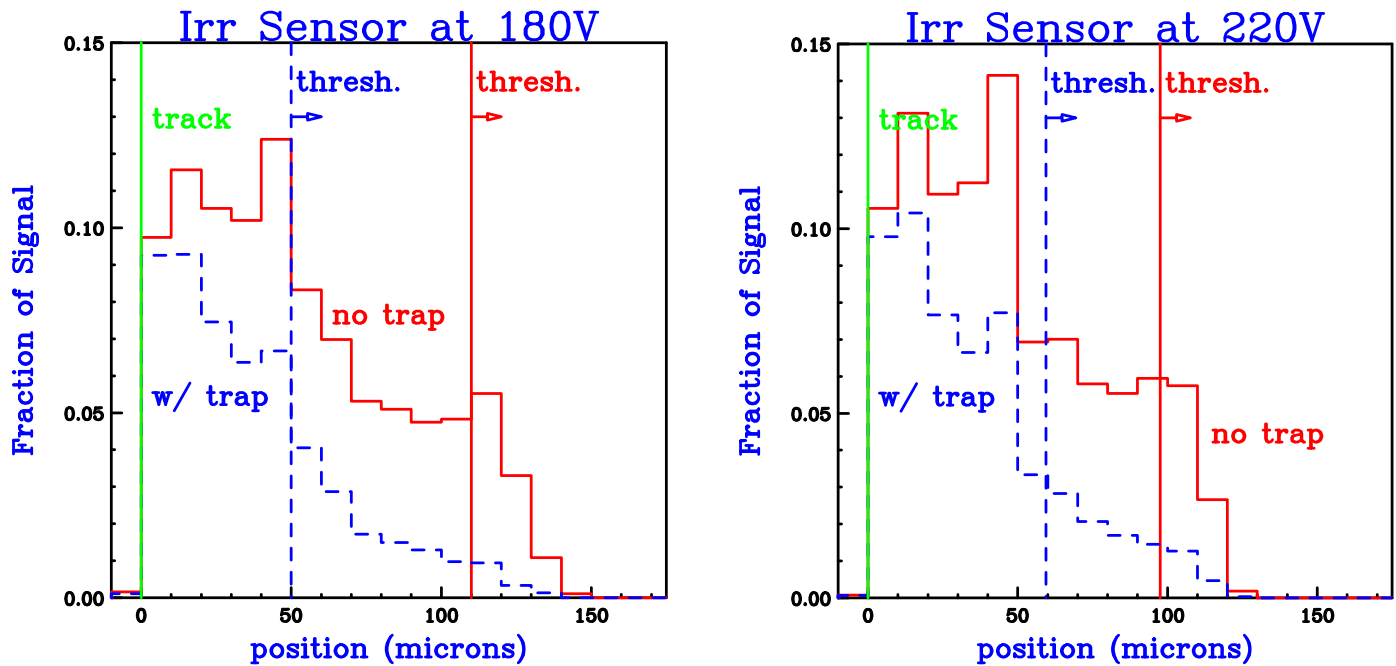


To study the transverse displacements of charges, it is convenient to avoid the strong focusing at the edges of the n+ implants: large single diodes are considered. The trajectories of a few single charges along a track are



- The total y displacement for e drift across the entire diode should be the same for normal and type inverted cases ($\int E dz$ is the same). → **It is!**
- The average electric field for electrons originating closer to the n+ side is smaller for the n-doped bulk than for the p-doped bulk
→ y of intermediate electrons is larger for new sensor than for irradiated sensor with same depletion voltage
- The transverse distribution of the electrons from a normally incident track is “broader” for the new sensor
 - Threshold requirement implies that new sensor has more charge sharing
 - y distribution is not flat as would be expected from constant Lorentz-angle. → **Constant Lorentz-angle simulations do not describe real charge sharing fcn!**

In real irradiated sensors, the trapping of carriers cannot be ignored. Turning-on the trapping removes electrons from the p+ implant side of the detector which have the largest transverse displacements:



The trapping probability decreases with increasing voltage but the Lorentz-angle also decreases with increasing voltage. Therefore, there is an optimum operating voltage for irradiated sensors that is larger than the full depletion voltage,

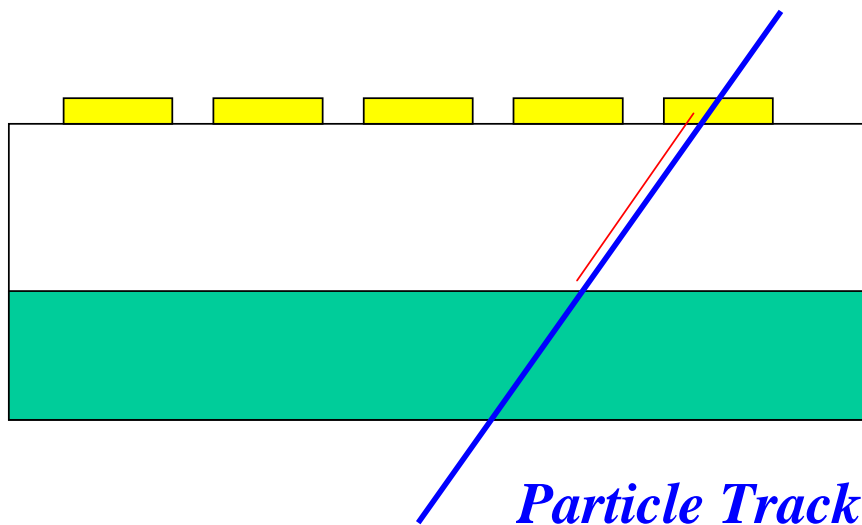
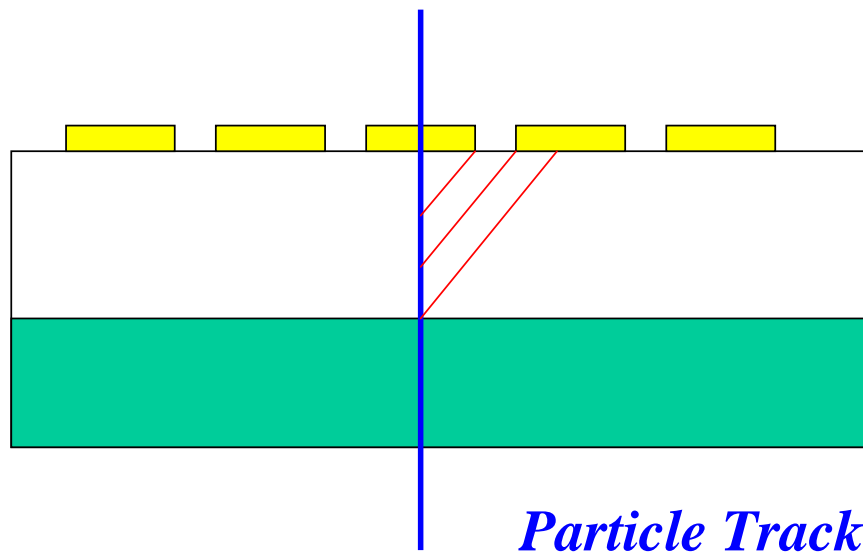
Voltage	No trap: Δy (90%)	W/ trap: Δy (90%)
180 V	110.0 μm	50.0 μm
220 V	97.6 μm	59.4 μm
260 V	87.6 μm	57.6 μm
300 V	80.0 μm	56.0 μm
500 V	54.8 μm	41.8 μm

→ Optimal voltage for this sensor is approximately 220 V

Atlas Results

At Vertex 99, F. Ragusa (Atlas Collaboration) presented a measurement of charge sharing in irradiated Atlas 400X50 micron detectors. The results were characterized by an effective Lorentz angle that was measured by determining the projected angle that minimized the cluster size,

- *measure the mean cluster length as function of the track incidence angle*

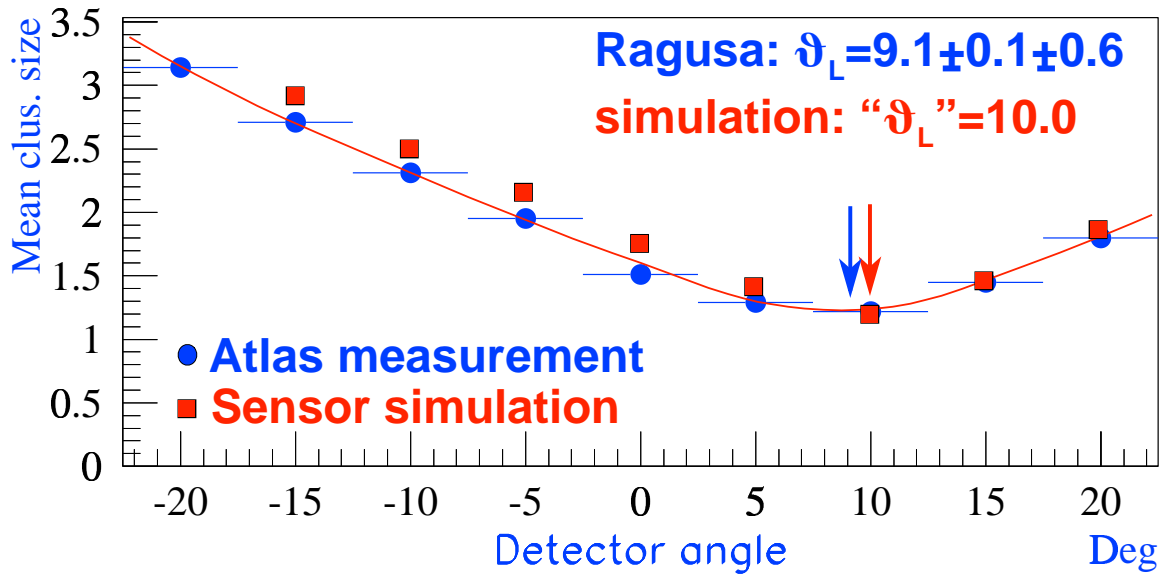


We have simulated their measurement despite some ignorance of many details:

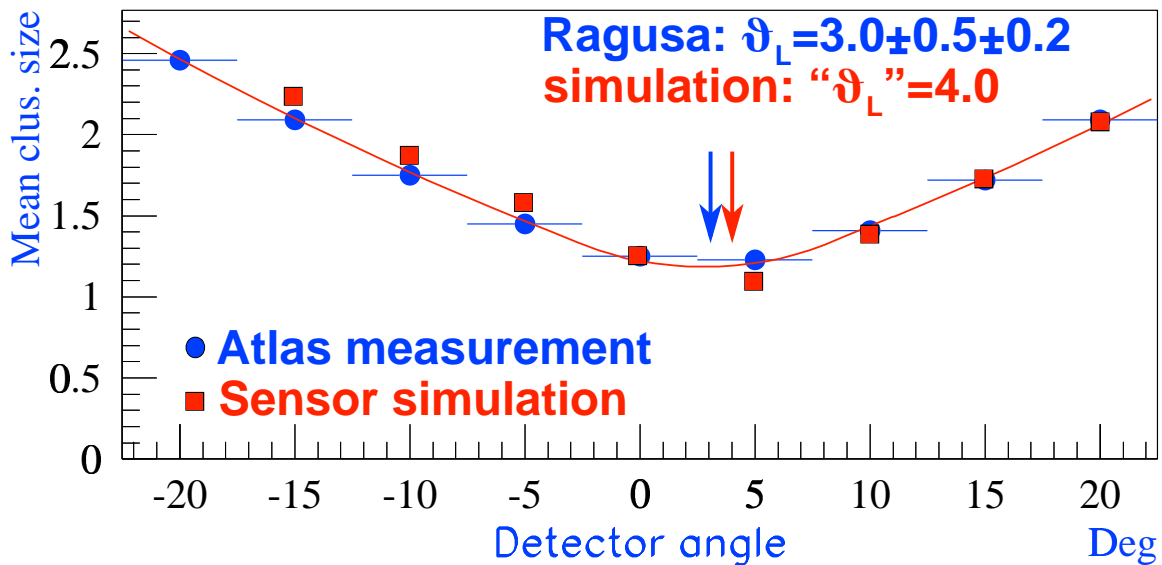
- 1. Don't know the initial resistivity of the material.**
- 2. Don't know the temperature of the sensors.**
- 3. Don't know the thresholds of the electronics (important for clust size).**
- 4. Don't know the thresholds of the electronics (important for clust size).**
- 5. Hall factor is uncertain at the 10-20% level.**
- 6. Atlas sensors were reported to have charge collection problems: 100% collection efficiency in simulation.**
- 7. Data selection criteria are not specified.**
- 8. Beam has broad angle spread (from error bars), simulation had delta-fcn angle spread.**

Note that the simulation is not “tuned” in any way. There are no free parameters. We compare our simulation directly with the published measurements:

ST2 non irradiated



IT2 -600 V: irr. 5×10^{14}



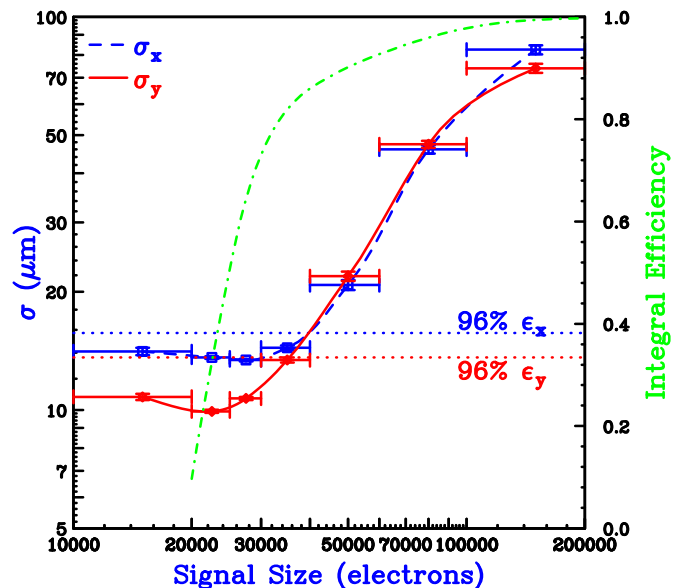
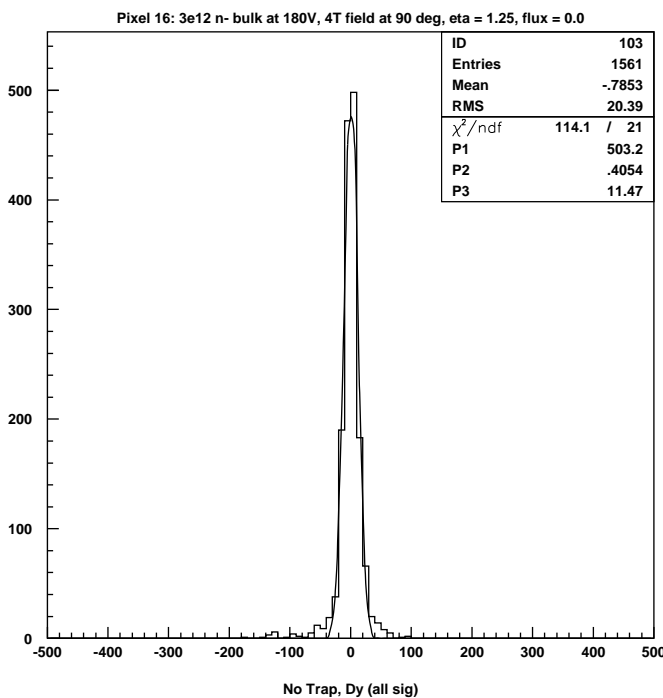
Flux	Measured θ_L	Sim θ_L
0	$9.1 \pm 0.1 \pm 0.6$	10.0 ± 1.0
5×10^{14}	$3.0 \pm 0.5 \pm 0.2$	4.0 ± 0.4
1×10^{15}	$3.2 \pm 1.2 \pm 0.5$	3.1 ± 0.3

Note that the simulation agrees well with the Atlas results

....

Hit Resolution

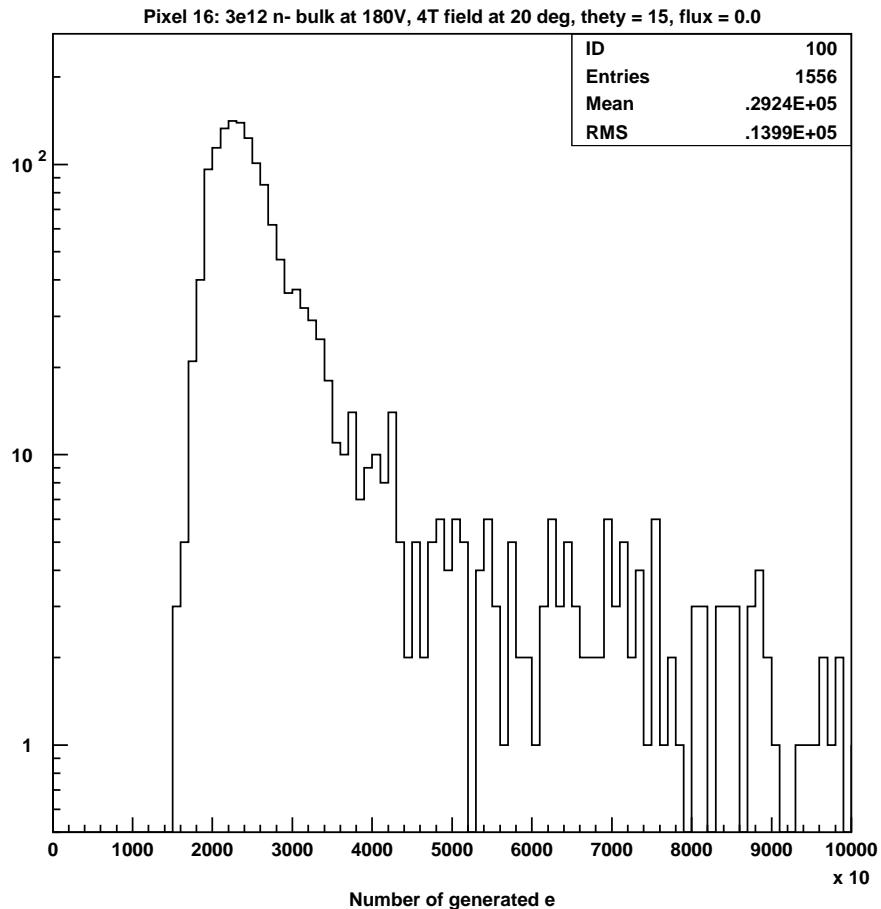
Resolution functions have, in general, complicated shapes and can be difficult to compare with one another. We categorize them in terms of single parameters but must be careful when doing so: the Gaussian half-width determines the “core” resolution but is insensitive to distribution “tails”, RMS is very sensitive to tails



can quote resolutions differing by a factor of 2! If there were no additional information, the RMS values would be a more meaningful measure of resolution. However, there is a correlation of resolution with signal size: **we can distinguish well-measured hits from poorly-measured ones. Choose to quote RMS for 96% of smallest signals.** Provides a resolution that is intermediate between the Gaussian and RMS extremes.

ROC Response Effects

The small fan angle of the forward blades produces much less charge sharing in the FPix than in the barrel. The most probable signal size in the forward detectors is approximately **22,000** electrons,



and the average signal size is approximately **30,000** electrons. Since the ROC analog response becomes non-linear near 20,000 electrons and saturates above 30,000 electrons, it seemed likely that the ROC would compromise the FPix resolution.

The simulated resolutions for 150×150 barrel and forward pixels (in μm , stat errors are $\sim 0.5\mu\text{m}$):

η	Low Dyn Rng		High Dyn Rng		Perf Resp	
	σ_x	σ_y	σ_x	σ_y	σ_x	σ_y
0.00	40.8	16.1	41.0	16.4	40.7	16.9
0.25	24.0	15.6	25.0	16.5	25.4	17.2
0.50	15.9	15.6	17.1	16.1	17.4	15.6
1.00	19.4	15.0	19.8	14.5	20.8	16.5
1.25	21.7	12.8	23.0	14.3	23.1	16.3
1.50	23.3	12.8	24.3	13.2	27.3	18.9
2.00	27.6	19.1	27.3	19.7	29.6	23.7
FPix	21.7	16.9	21.7	17.6	21.8	17.8

- x -resolution:

- Short Clusters at $\eta = 0 - 0.75$: improves with η
- Long Clusters at $\eta \geq 1.0$: signals in end pixels don't increase with η , δ -rays worsen resolution at large η

- y -resolution: use whole cluster, competing effects:

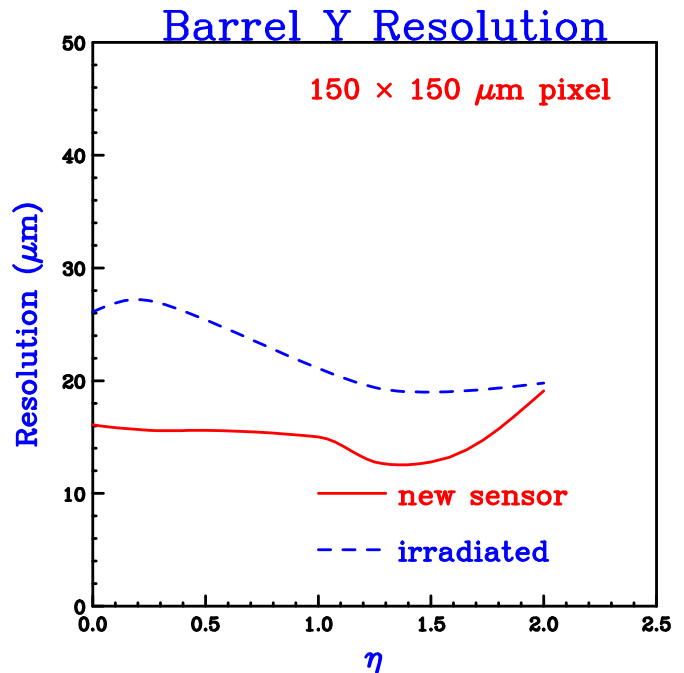
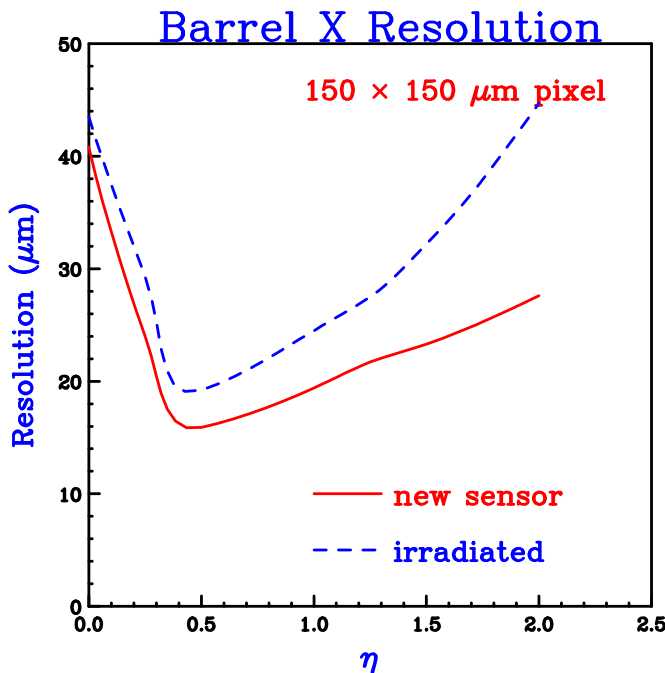
- Signal increases with η : improves resolution
- δ -emission increases with η : worsens resolution
- At very large η : δ s win

- All resolutions are best with Low Dynamic Range!

- Suppresses large fluctuations due to δ s
- Postpones the increase of σ_y with η
- Suggests that offline “trimming” of pixel signals might improve resolution even more!
- No reason to increase ROC linearity, even for FPix!

Baseline Pixel Resolutions

The 96% $x(z)$ and $y(\phi)$ barrel resolutions for new and irradiated sensors composed of $150 \times 150 \mu\text{m}$ pixels are



- Statistical uncertainties are typically $0.5 \mu\text{m}$
- σ_x ranges from $16 \mu\text{m}$ to $24 \mu\text{m}$ over most of the barrel and increases by $\sim 30\%$ after irradiation
- σ_y ranges from $13 \mu\text{m}$ to $16 \mu\text{m}$ over most of the barrel and increases by $\sim 50\%$ after irradiation
 - Note that a 96% $\sigma_y = 13 \mu\text{m}$ corresponds to a Gaussian fit resolution of $10 \mu\text{m}$.

The 96% $x(\phi)$ and $y(r)$ FPix resolutions for new and irradiated sensors composed of $150 \times 150 \mu\text{m}$ pixels are

Description	$N_{eff} (\text{cm}^{-3})$	Bias	Depl	Trp Q	σ_x	σ_y
New	-3×10^{12}	180 V	100%	0%	21.6	16.9
New	-3×10^{12}	220 V	100%	0%	20.7	17.3
Irr., norm	$+8.5 \times 10^{12}$	300 V	81%	46%	27.9	28.7
Irr., norm	$+8.5 \times 10^{12}$	500 V	100%	35%	23.6	22.1
Irr., oxy	$+3 \times 10^{12}$	220 V	100%	42%	25.8	25.0
Irr., oxy	$+3 \times 10^{12}$	300 V	100%	39%	25.4	23.2
Irr., oxy	$+3 \times 10^{12}$	500 V	100%	35%	22.9	22.3

- Statistical uncertainties are typically $0.5 \mu\text{m}$
- Charge sharing in the $x(\phi)$ direction is purely geometrical and improves in irradiated sensors at the largest voltages where the trapping is minimized
- Charge sharing in the $y(r)$ direction is a combination of geometrical and Lorentz drift. In irradiated sensors, it is also optimized at the largest voltages.
- Irradiation causes a resolution loss of $\sim 20\%$ in the x direction and $\sim 30\%$ in the y direction

Conclusions

- We have constructed a detailed Monte Carlo simulation of pixel sensors:
 - It incorporates “correct” charge deposition, electrostatics, charge transport, and trapping.
 - It agrees reasonably well with some limited test beam data and Atlas published results.
- It is being used to develop and tune pattern recognition and reconstruction algorithms.
- It is being used to study charge-sharing calibration.
- The analog saturation of the ROC **improves** the resolutions of both barrel and FPix
 - suppresses large fluctuations in deposited charge
 - offline “trimming” of individual pixel signals might further improve resolution
- The barrel resolutions with $150 \times 150 \mu\text{m}$ pixels are:
 - typically **16-24 μm** in x (z) and **13-16 μm** in y (ϕ)
 - a degradation of **30%** in x (z) and **50%** in y (ϕ) after an exposure of $6 \times 10^{14} \text{ h/cm}^2$ is expected if oxygenated Si works well.

- The FPix resolutions with $150 \times 150 \mu\text{m}$ pixels are:
 - typically **21 μm** in x (ϕ) and **17 μm** in y (r)
 - a degradation of **20%** in x (ϕ) and **30%** in y (r) after an exposure of **$6 \times 10^{14} \text{ h/cm}^2$** is expected if oxygenated Si works well and high voltage operation is possible.